JOURNAL OF MAGNETIC RESONANCE **124,** 87–96 (1997)
ARTICLE NO. MN961006

Double-Stacked Dielectric Resonator for Sensitive EPR Measurements

MAREK JAWORSKI,* ANDRZEJ SIENKIEWICZ,*† AND CHARLES P. SCHOLES‡

*Institute of Physics, Polish Academy of Sciences, Al. Lotników 32/46, 02-668 Warsaw, Poland; and ‡Chemistry Department, State University of New York at Albany, 1400 Washington Ave., Albany, New York 12222

Received July 5, 1996

A new approximate method for predicting the resonant frequencies and for solving the field distribution problem of a cylindrical dielectric resonator (DR) is developed. The model proposed in this paper bridges the gap between rigorous and accurate finite-element or Green function-based numerical methods on the one hand and on the other hand, simple approximate solutions in which the field distribution can be described analytically, but the resulting frequency is accurate within a few percent only. In the method described here, the approximate solution for the microwave field distribution is modified by substituting different values of the radial separation constants inside and outside of the disk-shaped DR. The model is generalized for the double-stacked DR structure and enables one to introduce corrections that take into account the presence of the shielding walls and of the cylindrical sample hole. Good agreement is found between experimental and calculated results for both the single and double-stacked structures that are designed around commercially available X-band DRs (9–10 GHz). For the resonant frequency of the lowest transverse-electric $TE_{01\delta}$ mode that is commonly used for EPR measurements, the accuracy of the method is better than 1%. Experimentally measured resonator filling factors are also in good agreement with those theoretically estimated. Both the theory and the experimental results suggest that the double-stacked DR structure with finite spacing between the ceramic cylinders is the most suitable for EPR measurements of long lossy samples.

INTRODUCTION

It has been stated long ago by Richtmyer (*1*) that nonmetallized dielectric objects can function as resonators. The actual technical applications of dielectric resonators (DRs) started in the late 1970s when temperature-stable, low-loss, high ϵ_r dielectric ceramic materials, such as barium tetratitanate, were becoming available (*2, 3*). Since that time, other composites with improved properties have been developed and the DR-related design is currently the basis of the whole segment of microwave industry where typical applications include microwave oscillators, narrowband microwave filters, radar detectors, speed guns, cellular telephones, and space telecommunication systems (*4, 5*).

† Also: Chemistry Department, State University of New York at Albany, 1400 Washington Ave., Albany, New York 12222.

Generally, implementation of ceramic DRs results in a substantial size reduction of microwave resonant structures. Since the high dielectric confines the electromagnetic fields to its own geometry rather than to the external metallic case, the size reduction is roughly proportional to the inverse square root of the dielectric constant (i.e., $1/\sqrt{\epsilon_r}$). Miniature resonant structures that contain DRs can also be an invaluable tool for probing signals in electron paramagnetic resonance spectroscopy, where hollow metallic cavities are commonly used to enhance the sensitivity of measurements. Due to their compactness, the DR systems exhibit much higher density of the electromagnetic energy stored inside the resonator. Thus, for the appropriately chosen field pattern (the resonant mode), one can concentrate the magnetic-field component ($\mathbf{H}_1$) at the sample position. This leads to a considerable improvement of the resonator filling factor η, which is an important design-related feature of the EPR probe head. Additionally, because of the low-dielectric loss of ceramics ($\tan\delta \sim 10^{-5}$ at 10 GHz), the quality factor Q of the free-running DR is high and comparable to that of a conventional cavity resonator. This is in contrast to other microwave noncavity resonators, such as miniature coils (*6*) or loop–gap resonators (LGRs) that are known for concentrating the magnetic field at the sample space and for having high filling factors η (*7*). Since the overall signal-to-noise ratio (S/N) of an EPR system is proportional to the product of η and Q (*8*), sensitivity improvement of more than two orders of magnitude compared to the standard TE_{102} cavity has already been reported while using the DR-based EPR probe for small, low-loss ''point'' samples (*9*).

The presence of high-loss (aqueous) samples distorts the microwave field inside the EPR resonators (*10*). The results already published suggest that the impact of lossy samples on the microwave characteristics of DR-type resonators is smaller than in the case of cavity resonators and LGRs. When loaded with high-loss samples contained in thin capillaries, the DR-based structures exhibit a relatively small decrease of the resonator Q factor and only a negligible shift of the resonant frequency (*9, 11*). This is because the high-dielectric ceramic leads to an essential redistribution of the magnetic and electric components of the microwave field.

1090-7807/97 $25.00

For the most commonly used disk-shaped DR with a vertical hole up the middle and operating in the lowest transverse-electric $TE_{01\delta}$ mode, the magnetic component $\mathbf{H}_1$ will be concentrated along the vertical axis where the sample is located, whereas the electric component $\mathbf{E}_1$ will be mostly confined within the dielectric disk. Therefore, these systems effectively isolate the electric component from the sample space and can be used as alternatives to metallic hollow resonators and LGRs for EPR studies of high-loss biological materials, particularly when the samples are limited in supply and sensitivity problems require obtaining the best S/N possible.

Several different versions of DR-type EPR resonators have been reported so far. Dykstra and Markham presented a DR for sensitive measurements of small point samples and liquid samples where a single DR surrounded by a microwave shield was movable in order to obtain precise matching to the external microwave circuit (*9*). Sienkiewicz *et al.* described a double-stacked DR structure that in combination with the stopped-flow technique has proven its adequacy for measurements of high-loss liquid samples where both a high S/N ratio and independence of flow-induced transients were the most critical points (*11*). A sensitive DR-type resonator containing a single disk made of high-dielectric ceramics and operating at cryogenic temperatures was designed by Walsh and Rupp (*12*). Bromberg and Chan took advantage of the open structure of a double-stacked DR and combined the resonator with a diamond anvil cell (DAC) that was located in the space between the ceramic disks for generating high hydrostatic pressures inside the resonant structure (*13*). An easy way of coupling the DR to the standard TE_{102} cavity has recently been proposed by Del Monaco *et al.* (*14*). The estimated ηQ product for this structure was found to be essentially higher than that for standard metallic cavities.

These examples indicate that the resonant structures designed around the DRs can find applications in different types of EPR experiments. Moreover, by using either single or double-stacked DR configurations it is possible to design resonant structures that exhibit slightly different microwave and geometric characteristics. This permits one to obtain an easier and more versatile fit of the DR-type resonator to the particular EPR application.

The major objective of the present work was to characterize the microwave parameters of the double-stacked DR structure from the point of view of its applications for EPR. In this paper, in order to develop our theoretical approach, we treat the single DR-based structure first. Then, we generalize the method to the double-stacked structure. In both cases we take into account the experimental results of microwave and EPR measurements performed using the DR-type resonators. As a result, we present a simple theoretical model enabling one to estimate the resonant frequency f_0 of the fundamental $TE_{01\delta}$ mode of the single and double DR-based structures that are designed around commercially available high-dielectric ceramic disks or cylinders. In the microwave X band, which is typical for the great majority of EPR experiments, this model yields an accuracy for f_0 that is better than 1%. The resonant-frequency problem is further developed for the case of two stacked DRs with a finite separation s between the ceramic disks, and the variation in f_0 as a function of s is discussed. A perturbation method enabling one to determine the resonant-frequency shift due to the presence of a cylindrical hole (sample space) in such a ceramic disk is also presented for both the single and double-stacked configurations. We also discuss the relative changes in the resonator quality factor Q for DRs loaded with samples having a high dielectric loss (aqueous samples). Considering the theoretical and experimentally observed filling factors, the advantageous properties of the double-stacked DR configuration for measuring lossy liquid samples contained in long capillaries are shown. The highest filling factor for such samples can be obtained in the double-stacked DR with a finite spacing between the dielectric cylinders.

EXPERIMENTAL

In this work we studied the single and double-stacked DR configurations that were designed around the commercially available X-band high-dielectric ceramics from two suppliers: Trans-Tech, Inc., Adamstown, Maryland, and MuRata-Erie North America, Inc., R/F Microwave Products, State College, Pennsylvania. Throughout this paper these ceramics will be referred to as Type I and Type II, respectively. The Type I ceramic (Trans-Tech Part No. C8733-0245-X-110-B-040) had dimensions of 6.22 mm o.d., 1 mm i.d., and 2.8 mm thickness. The dielectric constant ϵ_r of this material was 29.4. The Type II ceramic (MuRata-Erie Part No. DRT065R020C029) had dimensions of 6.55 mm o.d., 2 mm i.d., and 2.95 mm thickness. The corresponding dielectric constant ϵ_r was 29.2.

We configured our DR structures using the microwave heart of the system described in detail in Ref. (*11*). We used a microwave shield that was cylinder-shaped and made of a low-dielectric loss plastic, Rexolite (C-LEC Plastic, Inc., Beverley, New Jersey, Rexolite 1422, $\tan\delta = 6.6 \times 10^{-4}$, $\epsilon_r = 2.53$). The outer wall of the microwave shield was metallized with a few micrometers of silver plating. The microwave shield easily accommodated either one or two stacked DRs. In both cases, the DRs were centrally positioned with their axis aligned with the cylindrical axis of the microwave shield. The coupling to the external microwave circuit was achieved using a laterally protruded loop-shaped antenna. Since the antenna was adjacent to the side wall of the DR and its plane was perpendicular to the DR's cylindrical axis, a symmetrical $TE_{01\delta}$ mode could be excited for both the single and double-stacked structures. This type of coupling arrangement also made it possible to orient the plane of the antenna *parallel* to the cylindrical axis of the

microwave shield. In such orientation, the coupling loop preferentially excited the TM modes. This configuration was used while we checked our double structures for the presence of the nearest spurious TM modes.

While using the same microwave shield, it was possible to change the resonant frequency of the double-stacked structure by inserting spacers between the DRs. The spacers were also made of low-loss Rexolite plastic. Their thickness was carefully controlled in order to obtain the desired shift of the resonant frequency. This simple arrangement revealed a satisfactory reproducibility of setting the resonant frequency and was used for tuning the DR-based structures resonating in both the TE and TM modes.

The measurements of the resonance frequency and of the loaded and unloaded quality factor Q of the resonant structures were performed using a HP 8690B sweep oscillator. Q factors were determined from $f_0/\Delta f$, where Δf is the 3 dB bandwidth.

We compared the sensitivity of both the DR and the comercially available TE_{102} ST4102 resonator from Bruker. Both resonators contained the same testing samples. The measurements were performed on a Bruker ER 200D EPR spectrometer with a GaAsFET X-band amplifier before the crystal detector.

We used two types of samples. The first was a point 2,2-diphenyl-1-picrylhydrazyl (DPPH) sample whose linear dimension was less than 0.2 mm, and the second was a long liquid sample that was contained in a quartz capillary of 0.84 mm o.d. and 0.6 mm i.d. The latter sample was an aqueous solution of 4-hydroxy-2,2,6,6-tetramethylpiperidine-1-oxyl (TEMPO-OH). The total length of the aqueous sample was 3 cm, so it could fill the total active volume available for both resonators. The length of that active volume was 14 mm for the DR-based structures and 23 mm for the TE_{102} cavity, respectively. The point-DPPH sample was also used to study the axial distribution of the magnetic component H_z in the DR-based structures.

CALCULATION OF THE RESONANT FREQUENCY FOR SINGLE AND DOUBLE-STACKED DRs

For a disk-shaped dielectric resonator, commonly used in microwave applications, a closed-form analytical solution for the field distribution and the resonant frequency does not exist. Instead, one must use approximate methods, which can be roughly divided into two distinct groups: (i) rigorous and very accurate numerical procedures based on finite-element (*15*) or Green function formalism (*16*); and (ii) simple approximate models (*2, 17–19*), in which the field distribution can be described analytically, but the resulting resonant frequency is accurate within only a few percent (corresponding to hundreds of megahertz in the X band).

The model presented here has been developed to bridge the gap between these two approaches. From one side, the field distribution is still described by approximate analytical formulae. From the other side, owing to important modifications based on rigorous experimental results (*11, 20*), it is possible to calculate resonant frequencies within an accuracy of better than 1%. The resonant structure that contains a single dielectric resonator is discussed below in detail. Next, the results are generalized for the double structure, which is the central topic of this paper.

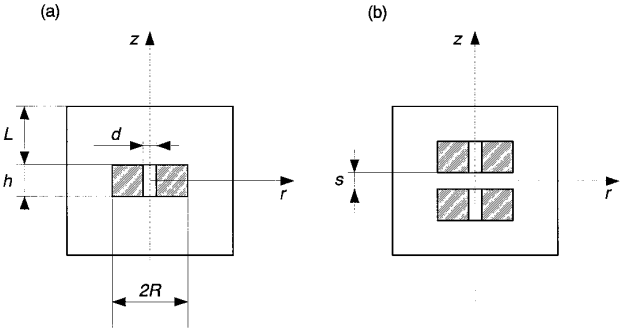

FIG. 1. Outline of the DR-based resonant structures studied. (a) Single DR-type resonator. (b) Double-stacked DR structure.

Let us first consider a dielectric disk of radius R and height h placed at the origin of the cylindrical coordinate system (r, ϕ, z). A schematic view of the corresponding resonant structure that is based on a single DR is shown in Fig. 1a. The expressions describing the fields $\mathbf{E}_1$ and $\mathbf{H}_1$ inside the dielectric disk follow directly from solution of the Maxwell equations in cylindrical coordinates. Outside of the dielectric, we assume the fields to vanish rapidly, so that, to a first approximation, the influence of the shielding walls can be neglected. The relevant parameters of the solution, i.e., propagation constants, dispersion parameters, follow from the boundary conditions on the interface dielectric-surrounding medium. In the next step, we will also take into account the presence of the metallic shield by imposing additional boundary conditions on the fields outside the dielectric disk.

In particular, for the fundamental $TE_{01\delta}$ mode of axial symmetry, within the dielectric medium ($|z| < h/2$, $r < R$), we have

$$\mathbf{E}_1 = \mathbf{i}_\phi E_\phi = \mathbf{i}_\phi J_1(\beta r)\cos\,\gamma z, \qquad [1a]$$

$$\mathbf{H}_1 = \mathbf{i}_r H_r + \mathbf{i}_z H_z = \frac{i}{\omega\mu}\,[\mathbf{i}_r \gamma J_1(\beta r)\sin\,\gamma z + \mathbf{i}_z \beta J_0(\beta r)\cos\,\gamma z], \qquad [1b]$$

and outside of the dielectric ($|z| > h/2$, $r < R$)

$$\mathbf{E}_1 = \mathbf{i}_\phi E_\phi = A\mathbf{i}_\phi J_1(\beta r)e^{-\alpha z}, \qquad [1c]$$

$$\mathbf{H}_1 = \mathbf{i}_r H_r + \mathbf{i}_z H_z = \frac{i}{\omega\mu}\,[A\mathbf{i}_r \alpha J_1(\beta r)e^{-\alpha z} + A\mathbf{i}_z \beta J_0(\beta r)e^{-\alpha z}], \qquad [1d]$$

where $\alpha = \sqrt{\beta^2 - k^2}$; $\gamma = \sqrt{\epsilon_r k^2 - \beta^2}$; $k = \omega/c$; $\omega = 2\pi f_0$; f_0 denotes the resonant frequency; ϵ_r is the dielectric permittivity; β is the radial separation constant; J_0 and J_1 are the zeroth- and first-order Bessel functions, respectively; and A is an unknown amplitude of the electromagnetic field.

Continuity conditions for the tangential components of the $\mathbf{E}_1$ and $\mathbf{H}_1$ fields at $|z| = h/2$ yield

$$\cos \gamma h/2 = Ae^{-\alpha h/2}, \quad \gamma \sin \gamma h/2 = A\alpha e^{-\alpha h/2}. \quad [2]$$

Hence, on eliminating the amplitude A we obtain the transcendental equation determining the propagation constant k, and consequently the resonant frequency f_0:

$$\gamma \tan \gamma h/2 = \alpha. \quad [3]$$

Comparing various models discussed so far in the literature (*2, 17–19*) one can find equations that are formally equivalent to Eq. [3], but with different boundary conditions for the lateral interface $r = R$. In particular, it turns out that the radial separation constant β is dependent on the adopted model and its value strongly affects the calculated resonant frequency. Thus, the proper choice of β is crucial for obtaining a satisfactory accuracy of the method.

Analysis of the rigorous solution (*16*) shows that the field distribution for $|z| > h/2$ is similar to that in the magnetic-wall model (*17*), while the field distribution within the dielectric is closer to the dielectric-waveguide model (*18*). Taking into account the above-mentioned arguments, one can modify Eq. [3] by substituting different values of the radial separation constants within the dielectric and outside of it,

$$\gamma = \sqrt{\epsilon_r k^2 - \beta_\epsilon^2}, \quad \alpha = \sqrt{\beta_0^2 - k^2}, \quad [4]$$

where $\beta_0 = \kappa_{0,1}/R$ and $\kappa_{0,1} = 2.4048$ denotes the first root of the Bessel function $J_0(\beta r)$.

The radial separation constant within the dielectric β_ϵ can be determined from the dielectric-waveguide model (*18*) by matching the fields E_ϕ and H_z on the interface at $r = R$. From the continuity condition we find

$$\beta_\epsilon \frac{J_0(\beta_\epsilon R)}{J_1(\beta_\epsilon R)} = -\mu \frac{K_0(\mu R)}{K_1(\mu R)}, \quad [5]$$

where $\mu = \sqrt{(\epsilon_r - 1)k^2 - \beta_\epsilon^2}$, J_0 and J_1 denote Bessel functions, and K_0 and K_1 are modified Bessel functions of the second kind. For small variations of β, the matching formula Eq. [5] can be linearized in the vicinity of β_0, yielding

$$(\beta_\epsilon R)^2 = C_1(\epsilon_r - 1)(kR)^2 + C_2, \quad [6]$$

where C_1 and C_2 are constants.

In the dielectric-waveguide model, the values of β_ϵ resulting from Eq. [5] are slightly higher than β_0 and the realistic range of $\beta_\epsilon R$ can be estimated to be $\beta_\epsilon R \in (2.5, 2.8)$. For this range of $\beta_\epsilon R$ the linearization of Eq. [5] yields numerical values $C_1 = 0.35$, $C_2 = 4.21$. In the dielectric resonator, however, due to the finite height h, the field concentration within the dielectric will be dependent on the resonator dimensions, giving rise to the dependence of β_ϵ on the ratio $h/2R$. Generally, this leads to smaller values of β_ϵ.

Taking into account a set of accurate experimental results (*20, 21*) obtained for the DRs having $\epsilon_r \simeq 30$ and for various ratios $h/2R$, one can introduce a ''semiempirical'' formula in the form of Eq. [6], but with $C_1 = 0.145$, $C_2 = 5.93$. The smaller slope C_1 of the semiempirical formula (as compared to that resulting from the dielectric-waveguide model) reflects to some extent the dependence of β_ϵ on the resonator dimensions $h/2R$.

So far we have considered the fields outside of the DR disk to vanish exponentially for $|z| > h/2$. If we take into account the presence of the shielding walls, we should impose the boundary conditions at $|z| = h/2 + L$, where L denotes the distance between the DR disk and the upper or lower lid of the cylindrical shield (see Fig. 1a). Consequently, the exponential dependence on the distance along the axial direction z in Eqs. [1c] and [1d] should be replaced by hyperbolic functions: $\sinh[\alpha(z - L)]$ for E_ϕ, H_z, and $\cosh[\alpha(z - L)]$ for H_r, respectively. Thus, for a single DR structure, the equation determining the resonant frequency f_0 takes finally the form

$$\gamma \tan \gamma h/2 = \alpha \coth \alpha L, \quad [7]$$

where α and γ are given by Eq. [4].

The presence of a lateral shield can be implicitly included in the semiempirical expression (Eq. [6]). It turns out, however, that for the typical range of parameters the fields vanish rapidly in the radial direction and the influence of the lateral shield can be neglected. Equations [6] and [7] form a system of nonlinear equations, which for given dimensions of the dielectric resonator and the permittivity of the dielectric medium can be solved for k and consequently for the resonant frequency f_0. One should stress, however, that the linearized formula Eq. [6] is valid only in the restricted range of parameters, i.e., for $\epsilon_r \simeq 30$, and $0.4 < h/2R < 1$, and that this is the price we pay for accurate results while keeping the calculations relatively simple. It should be noted here that for $\beta_0 \neq \beta_\epsilon$ the Maxwell equations are satisfied rigorously both in the dielectric region and in the surrounding medium. However, the boundary conditions for $z = h/2$ are satisfied only approximately.

The generalization of the calculation procedure for the double-stacked DR structure is straightforward and follows

closely the approach outlined above. The double structure of the dielectric resonator is shown schematically in Fig. 1b. In particular, the fields within the dielectric can be expressed as

$$\mathbf{E}_1 = \mathbf{i}_\phi J_1(\beta r)(A \sin \gamma z + B \cos \gamma z), \quad [8a]$$

$$\mathbf{H}_1 = \frac{i}{\omega\mu}[\mathbf{i}_r \gamma J_1(\beta r)(A \cos \gamma z - B \sin \gamma z) + \mathbf{i}_z \beta J_0(\beta r)(A \sin \gamma z + B \cos \gamma z)], \quad [8b]$$

while outside of the dielectric we have for $|z| > h + s/2$, $r < R$,

$$\mathbf{E}_1 = C\mathbf{i}_\phi J_1(\beta r)e^{-\alpha z}, \quad [8c]$$

$$\mathbf{H}_1 = \frac{i}{\omega\mu}[C\mathbf{i}_r \alpha J_1(\beta r)e^{-\alpha z} + C\mathbf{i}_z \beta J_0(\beta r)e^{-\alpha z}], \quad [8d]$$

and for $|z| < s/2$, $r < R$,

$$\mathbf{E}_1 = D\mathbf{i}_\phi J_1(\beta r)\cosh \alpha z, \quad [8e]$$

$$\mathbf{H}_1 = \frac{i}{\omega\mu}[-D\mathbf{i}_r \alpha J_1(\beta r)\sinh \alpha z + D\mathbf{i}_z \beta J_0(\beta r)\cosh \alpha z], \quad [8f]$$

where α and γ are given by Eq. [4]. As before, the presence of the shield can easily be included by replacing exponentials in Eqs. [8c] and [8d] by appropriate hyperbolic functions.

On matching the fields E_ϕ and H_r across the interfaces $|z| = s/2$ and $|z| = h + s/2$ and eliminating the amplitudes A, B, C, D, we obtain the transcendental equation

$$(\gamma + \alpha \coth \alpha L \tan \gamma h/2)(\alpha \tanh \alpha s/2 - \gamma \tan \gamma h/2) = (\gamma + \alpha \tanh \alpha s/2 \tan \gamma h/2) \times (\gamma \tan \gamma h/2 - \alpha \coth \alpha L), \quad [9]$$

TABLE 1

The Comparison of the Measured f_{0m} and Calculated f_{0c} Resonant Frequencies at Various Separations s of the DR Cylinders[a]

Separation s (mm)	f_{0m} (GHz)	f_{0c} (GHz)
0.00	8.256	8.265
0.65	8.647	8.660
1.35	8.920	8.945
1.60	8.994	9.020
2.00	9.080	9.118
2.50	9.200	9.211
3.00	9.260	9.282

[a] Type I ceramic.

TABLE 2

The Comparison of the Measured f_{0m} and Calculated f_{0c} Resonant Frequencies at Various Separations s of the DR Cylinders[a]

Separation s (mm)	f_{0m} (GHz)	f_{0c} (GHz)
0.00	8.050	7.970
1.50	8.700	8.640
2.00	8.810	8.760
3.50	9.060	8.990
4.00	9.120	9.050
4.50	9.190	9.100

[a] Type II ceramic.

which, with the help of Eq. [6], can be solved for k, i.e., for the resonant frequency f_0.

So far we have considered uniform dielectric disks of radius R and height h. The real resonator used for EPR measurements has a sample hole placed axially within the dielectric. Since the $\mathbf{E}_1$ field on the interface between the ceramic and the surrounding medium has only the tangential component, we can neglect the field distortion within the hole and evaluate its influence using the perturbation method. Assuming the $\mathbf{E}_1$ field distribution as in the uniform dielectric disk, we find

$$\frac{\Delta f_0}{f_0} = \left(1 - \frac{1}{\epsilon_r}\right)\frac{\int_{V_h} |\mathbf{E}_1|^2 dv}{2\int_{V_c} |\mathbf{E}_1|^2 dv}, \quad [10]$$

where V_h and V_c denote the hole and resonator volume, respectively, and the field $\mathbf{E}_1$ is given by Eq. [8]. Thus, the procedure for finding the resonant frequency f_0 consists of two steps. First, the resonant frequency of the double dielectric structure is computed using Eq. [9]. Next, the correction following from the perturbation formula Eq. [10] is taken into account.

The comparison of the measured and calculated resonant frequencies for various separations s is shown in Tables 1 and 2 for the two selected double-stacked DR structures. The presence of the low-loss Rexolite plastic around the DR disks has been included by taking $\epsilon_r = 2.53$ instead of $\epsilon_r = 1$ for the surrounding medium, in order appropriately to rescale Eqs. [4], [7], and [9]. The accuracy is better than 1% (corresponding to 100 MHz in the X band) and is independent of s, which indicates indirectly that Eqs. [8a]–[8f] approximate well the real field distribution. Figure 2 demonstrates the application of our method for predicting the resonant frequency of the $TE_{01\delta}$ mode for the double-stacked DR structure. Within the entire range of separations s from 0 to 3 mm, the theoretical curve for the resonant frequency (solid line) nearly overlaps the results measured experimentally (dashed line). The experimental data were

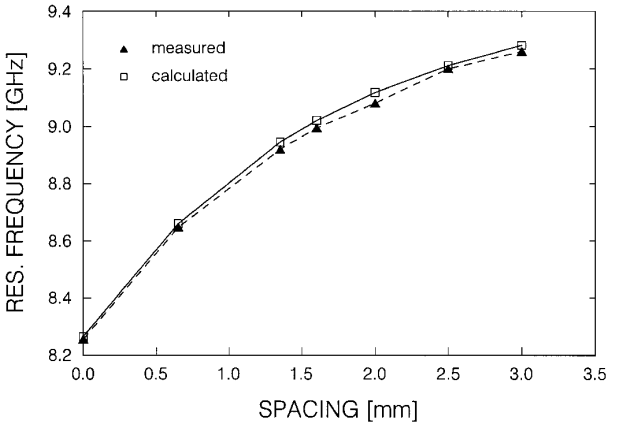

FIG. 2. The measured and calculated dependencies of the resonant frequency on the separation s for the double-stacked DR (Type I ceramic).

obtained for the resonant structures designed around the commercially available high-dielectric (Type I) ceramics.

The method of analysis outlined above is applicable to the fundamental $TE_{01\delta}$ mode. Generalization to the higher TE modes of axial symmetry is straightforward, although the accuracy of solution deteriorates as we increase the radial and longitudinal indices. Unfortunately, the analysis of the TM modes is much more difficult, mainly because of the discontinuity of the E_z component at the front wall of the dielectric resonator. For the same reason we cannot apply the perturbation formula (Eq. [10]), since the electric field E_z in the sample hole differs considerably from that in the uniform dielectric cylinder.

For a single dielectric resonator, the nearest spurious mode is of the TM type and its resonant frequency is above that of the $TE_{01\delta}$ mode as long as $h/2R < 1$ (*19*). However, for the double-stacked configuration with no separation between the DR cylinders we have $h/2R \sim 0.9$ and the system approaches the situation where the EPR-active $TE_{01\delta}$ mode may become degenerate with the TM mode.

In order to check the location of the spurious TM mode for the double structure, we measured the resonant frequencies of both the TE and TM modes at various separations s of the DR cylinders. The experimental data shown in Fig. 3 indicate that the TE/TM offset is ~400 MHz and is nearly constant over the entire range of s (0 to 4.5 mm). In this experiment, the resonant structures were designed around the Type II ceramic. For the EPR-active $TE_{01\delta}$ mode, changing the spacing from 0 to 4.5 mm gave about 1 GHz variation of f_0. It is important to note that, contrary to the other methods of tuning, such as inserting movable metallic or dielectric plungers, tuning by separation does not affect microwave characteristics of the DR-type resonator (*22*). In particular, the resonator quality factor Q remains practically constant.

EVALUATION OF THE FILLING FACTOR η AND THE QUALITY FACTOR Q

As mentioned above, the solution of Eq. [9] enables one not only to evaluate the resonant frequency but also to describe approximately the $\mathbf{E}_1$ and $\mathbf{H}_1$ distribution for the fundamental $TE_{01\delta}$ mode, both within the dielectric and in adjacent regions. Once the field distribution is known, one can evaluate several parameters that are important for the EPR measurements, such as the resonator filling factor η, total energy accumulated in the resonant structure, dielectric losses within a sample, and the resonator quality factor Q. In this paper we concentrate our attention mainly on the filling factor η and the quality factor Q.

According to Ref. (*23*), the filling factor for the magnetic field $\mathbf{H}_1$ is given by

$$\eta = \frac{\int_{V_s} |\mathbf{H}_{1\perp}|^2 dv}{\int_{V_c} |\mathbf{H}_1|^2 dv}, \qquad [11]$$

where V_s and V_c denote the sample and resonator volume, respectively, and the field $\mathbf{H}_1$ is given by Eq. [8].

It should be stressed that only the field component that is normal to the static magnetic field H_0 will contribute to the integral in the numerator of Eq. [11]. However, for typical sample dimensions (small point samples or thin capillaries) one can neglect the contribution from the radial component and integrate only H_z^2 over the sample volume.

The highest filling factor for point samples can be obtained in a single structure, for which the energy is concentrated in a small volume, and consequently, the field amplitude within a sample is higher. For a typical commercially available (Type I) ceramic with a loaded Q of ~2000, the magnetic-field amplitude is estimated to be as high as 20 G for 1 W of incident input power and the calculated filling factor is

$$\eta \simeq 0.036 V_s, \qquad [12]$$

where the sample volume V_s is given in cubic millimeters.

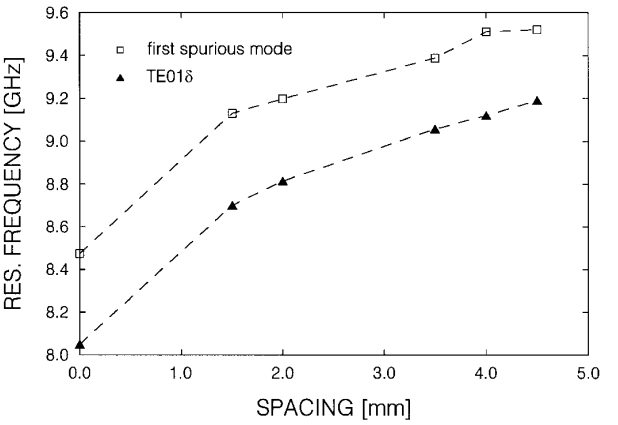

FIG. 3. Measured dependence of the resonant frequency on the separation s for the double-stacked DR. The EPR-active $TE_{01\delta}$ mode and the first spurious TM mode are shown (Type II ceramic).

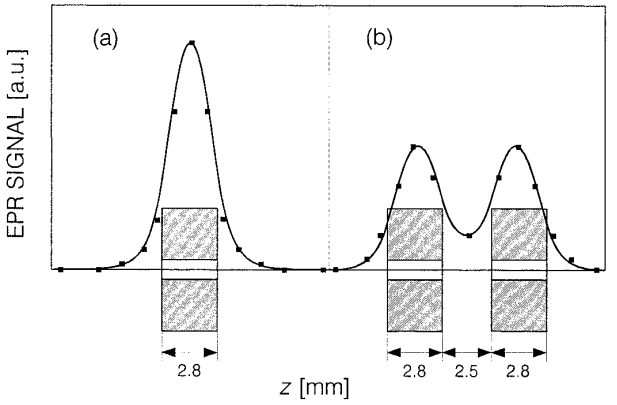

FIG. 4. The comparison of the relative estimated and measured EPR line intensities as a function of the point-DPPH sample position. (a) The relative EPR signal intensity for the point sample probing H_z^2 along the z axis of the single DR. (b) The relative EPR signal intensity for the point sample probing H_z^2 along the z axis of the double-stacked DR. The solid squares represent the experimental results, and the solid line depicts the estimated EPR signal intensity. Type I ceramic; for the double DR the separation s is 2.5 mm.

For comparison, the corresponding filling factor η estimated for the standard rectangular TE_{102} cavity is $0.0002V_s$ (*23*). Consequently, since the filling factor of the single DR (expressed by Eq. [12]) is roughly two orders of magnitude greater than that for the standard cavities, the DR should yield a much higher EPR signal intensity for small nonsaturable samples (*9*, *11*).

For the double-stacked DR structure resonating at the same frequency, and for the same incident microwave power, the energy is distributed over the larger volume, and the filling factor for the point sample decreases. For the double-stacked DR without separation of the ceramic cylinders ($s = 0$), the resonator filling factor for point samples is $0.025V_s$, i.e., roughly 30% lower than that for the single DR. The comparison of the predicted and measured EPR signal intensities for both the single and double DR-based structures is given in Fig. 4. The solid line depicts the estimated relative signal intensity that is plotted as a function of axial coordinate z (sample position). The solid squares represent the relative experimental EPR signal intensities measured for a point-DPPH sample that was moved along the length of the resonant structure. Figure 4a shows the comparison of the measured and estimated EPR signals for the single DR structure, whereas Fig. 4b compares these two sets of data for the double-stacked DR structure. For both types of DR structures the estimated signal intensity is in good agreement with the experimental results. The theoretical fit (solid line in Figs. 4a and 4b) was obtained by taking the appropriate values of $|\mathbf{H}_1|^2$ calculated from Eqs. [8b], [8d], and [8f].

Table 3 summarizes the dependence of the filling factor η as a function of separation s between the dielectric cylinders for the double-stacked DR structure and for a point sample positioned in two different locations: (i) in the resonator center and (ii) at the location where the H_z attains its local maximum ($H_{z,max}$).

TABLE 3
The Calculated Relative Filling Factor η/V_s (mm^{-3}) as a Function of Separation s for the Double-Stacked DR Structure[a]

Separation s (mm)	Point sample in the resonator center	Point sample located at $H_{z,max}$	Long sample[b]
0.00	0.0248	0.0248	0.0074
0.50	0.0187	0.0208	0.0077
1.00	0.0136	0.0191	0.0078
1.50	0.0099	0.0185	0.0078
2.00	0.0071	0.0181	0.0077
2.50	0.0050	0.0179	0.0076
3.00	0.0036	0.0179	0.0075

[a] Type I ceramic.
[b] Sample in a long capillary (0.64 mm i.d.).

The comparison of the EPR line intensities for the double-stacked DR and for the rectangular TE_{102} cavity is shown in Fig. 5. The EPR line intensities were measured for a small point-DPPH sample positioned exactly in the middle of both resonators. The line intensity observed for the double DR is roughly 30 times larger than that obtained in the TE_{102} cavity. This result is somewhat lower than predicted theoretically. However, the EPR spectrum presented in Fig. 5 was obtained for the point-DPPH sample located exactly in the middle of the double-stacked DR structure ($z = 0$, separation s of 1.3 mm). It can be seen from Fig. 4 that such a structure yields a lower intensity of EPR signals for small samples than a single DR. The energy of the microwave field is spread over a larger volume in the double-stacked DR structure and this

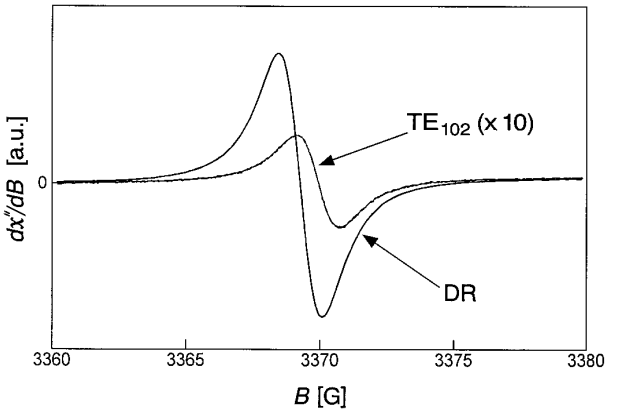

FIG. 5. EPR spectra of the point-DPPH sample measured in a double-stacked DR structure and in a standard TE_{102} cavity. The spectra were recorded with the same incident microwave power (0.2 mW) and with the same effective magnetic-field modulation (0.5 G).

results in lower intensity of the magnetic component that is sensed by a small DPPH sample. Actually, such a small sample probes $|\mathbf{H}_1|^2$ at its location inside the resonator (*13*). Assuming the same incident power for both single and double DR structures one should expect a lower signal intensity for the double-stacked DR. Thus, for small samples measured under nonsaturating conditions, a single dielectric resonator exhibits the largest filling factor and consequently the highest sensitivity among various structures studied in this work.

Contrary to the point samples, long capillaries are small in the radial direction but fill the entire distance between the upper and lower lids of the microwave shield. As a result, the field distribution along the symmetry axis strongly influences the filling factor η. Taking as an example the same (Type I) single dielectric resonator as before, we find

$$\eta \simeq 0.0065 V_s \qquad [13]$$

for the cylindrical microwave shield with a distance between the upper and lower lids of 14 mm and the sample volume V_s given in cubic millimeters. In the double structure, owing to the fact that the magnetic component H_z along the z axis is more evenly distributed, the resonator filling factors for long capillaries are slightly higher (roughly by 10%). Actually, for the double DR structure, we observe a further increase of η with increasing separation s. The calculated dependence of the relative filling factor on separation s for the double-stacked (Type I) DR and for a long capillary is summarized in Table 3. As a function of spacing s, the relative filling factor η increases slowly and attains a relatively broad plateau around s_{opt} of 1.1–1.5 mm. In particular, at $s \simeq 1.3$ mm we have

$$\eta \simeq 0.0078 V_s \qquad [14]$$

with V_s given in cubic millimeters, as before.

For the double-stacked DR structure with separation s of 1.3 mm and for a typical sample capillary (i.d. of 0.64 mm) the sample volume is of 4.5 mm^3. Hence, Eq. [14] yields $\eta \simeq 0.035$, while for the same kind of sample placed in the standard TE_{102} cavity the estimated η is of 0.0007. Thus, for a long capillary, the filling factor η is roughly 50 times larger for the double-stacked DR-type resonator than for the TE_{102} cavity. While estimating η for the rectangular cavity, we assumed that the total sample volume in the TE_{102} resonator was 7 mm^3, i.e., that the same long capillary (0.64 mm i.d.) was entirely filled with liquid sample and positioned along the active region of the cavity.

Figure 6 compares the EPR spectra obtained for 300 μM water solution of the nitroxide TEMPO-OH in the double-stacked DR and the TE_{102} cavity. The signal intensity was measured for a 3 cm long sample contained in a 0.6 mm i.d. quartz capillary inserted along the active volume of both resonators. For the same experimental conditions, the double-stacked DR yields an EPR signal intensity that is roughly 30 times larger than that in the TE_{102} cavity. This experimental result is in good agreement with the theoretical estimation of the filling factors η for both resonators. Since the Q factor of the DR-based resonator loaded with an aqueous sample is lower than that of the TE_{102} resonator, the actual gain in the EPR signal intensity is slightly lower than the ratio of the corresponding filling factors.

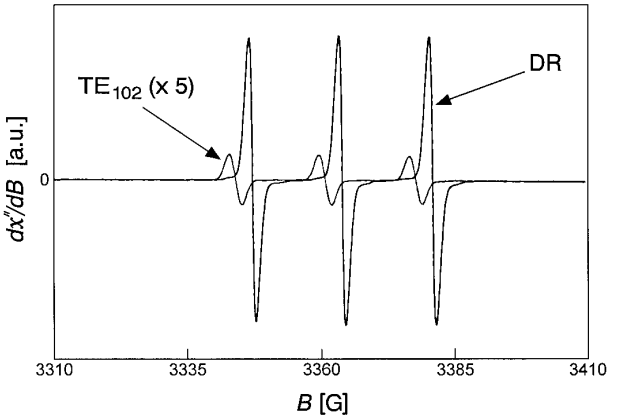

FIG. 6. EPR spectra for a long aqueous sample contained in a quartz capillary of 0.6 mm i.d., measured in a double-stacked DR structure and in a TE_{102} cavity. The spectra were recorded for the water solution of the nitroxide TEMPO-OH (300 μM) using the same experimental conditions: microwave power of 2 mW and the 100 kHz magnetic-field modulation of 0.1 G.

The results indicate that for liquid samples measured in long capillaries, one should expect the best S/N for the double-stacked structure with a finite separation s between the DRs. The optimum separation s_{opt} will depend on the dielectric constant ϵ_r, the dimensions of the DRs, and, to some extent, on the capillary inner diameter d_s. In particular, the double DR with a finite separation s of 1.1–1.5 mm between the ceramic cylinders seems to be the most suitable for EPR measurements of liquid samples since it has better overall field uniformity. This may also be an important factor while performing EPR measurements under saturating conditions.

For a lossy sample described by macroscopic parameters ϵ and σ (where σ denotes the conductivity of the material) one can calculate the average dielectric losses P_d,

$$P_d = \frac{1}{2}\int_{V_s} \sigma |\mathbf{E}_1|^2 dv, \qquad [15]$$

and the quality factor Q_ϵ,

$$Q_\epsilon = \frac{\omega W}{P_d} = \frac{\omega \int_{V_c} \epsilon |\mathbf{E}_1|^2 dv}{\int_{V_s} \sigma |\mathbf{E}_1|^2 dv}, \qquad [16]$$

TABLE 4

The Comparison of the Measured Q_m and Calculated Q_c Loaded Q Factors as a Function of the Capillary i.d. for the Double-Stacked DR[a] (Critically Coupled, the Capillary Filled with Water)

d_s (mm)	Q_m	Q_c
0.0	2400	2400
0.6	1460	1060
0.7	1171	718
0.8	742	480
1.0	291	223

[a] Type II ceramic.

where W denotes the total energy in the resonant structure, $\omega = 2\pi f$ is the angular frequency, and Q_ϵ is a hypothetical quality factor related only to dielectric losses within the sample. The total unloaded quality factor Q follows from the standard expression

$$\frac{1}{Q} = \frac{1}{Q_\epsilon} + \frac{1}{Q_0}, \qquad [17]$$

where Q_0 denotes the Q factor of the resonant structure without a sample.

Table 4 shows the comparison of the calculated (Q_c) and measured (Q_m) quality factors as a function of the sample diameter d_s. The corresponding double DR structure was designed around two ceramic (Type II) DRs with $s = 3.5$ mm and $Q_0 = 2400$. For the calculations we took the dielectric parameters of water from Ref. (*24*). Contrary to the results presented above for the resonant frequency and field distribution, the agreement between calculated and measured Q factors is now much worse. On one hand, the measurements of Q are less precise than those of the resonant frequency. On the other, there are systematic errors following from the simplifications made while deriving Eqs. [15] and [16]. Therefore, the results concerning dielectric losses, Q factors, etc., should be considered only as a rough estimate, and the agreement between theory and measurements is qualitative rather than quantitative.

It seems that the main source of the systematic error in Q-factor calculations is related to the assumption that the $\mathbf{E}_1$ field distribution within the sample volume is the same as in the uniform structure. Such a simplification was justifiable in the perturbation approach (Eq. [10]), where we calculated approximately a small correction to the resonant frequency. Now, however, we use the same field distribution to calculate an absolute value of Q (Eq. [15]), and the relative error is much greater than that in the case of the resonant frequency.

In particular, it seems that the presence of a quartz capillary affects the field distribution within an aqueous sample. Preliminary calculations indicate that the presence of a thin quartz wall diminishes the $\mathbf{E}_1$ field amplitude within the sample while keeping the $\mathbf{H}_1$ field unchanged. As a result, the dielectric losses are lower, and the quality factor is higher, in agreement with experimental data (Table 4).

CONCLUSIONS

In conclusion, we report that the semiempirical method presented in this paper provides a relatively simple and precise way for estimating the essential microwave characteristics of the DR type of resonator. Our theoretical model employs a combination of approximate analytical formulae with the rigorous experimental results obtained for a series of different resonant structures that were designed around either single or double DRs. This approach permits one to predict the technical parameters of the real resonant structures, since it takes into account the presence of a sample hole that often must be drilled in the dielectric disk, as well as introduces corrections for the presence of the metallic walls (the microwave shield). While estimating the resonance frequency of the lowest, EPR-active $TE_{01\delta}$ mode, this approach yields an accuracy that is better than 1% for the typical commercially available X-band DRs and for which $\epsilon_r \simeq 30$. It seems that this method gives a correct estimate for the distribution of electric and magnetic components inside the DR-based structure, since a fairly good agreement for the resonant frequency is found for the double-stacked DR structures that had various spacings between the DR cylinders.

From the point of view of EPR applications, the double-stacked DR system that is discussed in this paper offers several interesting features. While for point samples a higher filling factor η can be obtained in a single DR structure, the double-stacked DR with a finite separation between dielectric disks yields the best S/N ratio for long aqueous samples. In the double DR, the magnetic field $\mathbf{H}_1$ is more evenly distributed than in the single DR structure, which may be of importance while measuring saturable samples. It is easily tunable, and an almost linear tuning range of 15–20% is attainable without visible degradation of resonator characteristics. In a natural way, the double DR structure is also more transparent for photo-EPR experiments, making easier the introduction of light to the sample space.

ACKNOWLEDGMENTS

This work has been supported by NIH Grant GM 35103 and by the U.S.–Poland Maria Skłodowska–Curie Joint Fund II, PAN/NIST-94-203. We are also grateful to Mr. R. A. Isaacson, Department of Physics, UCSD, for many stimulating discussions at the beginning of this work and for providing us with some of his experimental results regarding single and double-stacked DRs.

REFERENCES

1. D. Richtmyer, *J. Appl. Phys.* **10,** 391 (1939).
2. S. B. Cohn, *IEEE Trans. Microwave Theory Tech.* **MTT-16,** 218 (1968).

3. J. K. Plourde, D. H. Linn, H. M. O'Bryan, Jr., and J. Thomson, Jr., *J. Am. Ceram. Soc.* **58,** 418 (1975).
4. J. K. Plourde and C. L. Ren, *IEEE Trans. Microwave Theory Tech.* **MTT-29,** 754 (1981).
5. R. R. Bonetti and A. E. Atia, *IEEE Trans. Microwave Theory Tech.* **MTT-29,** 1333 (1981).
6. H. Mahdjour, W. G. Clark, and K. Baberschke, *Rev. Sci. Instrum.* **57,** 1100 (1986).
7. W. Froncisz and J. S. Hyde, *J. Magn. Reson.* **47,** 515 (1982).
8. C. P. Poole, ''Electron Spin Resonance: A Comprehensive Treatise on Experimental Techniques,'' Chap. 11, Wiley–Interscience, New York, 1967.
9. R. W. Dykstra and G. D. Markham, *J. Magn. Reson.* **69,** 350 (1986).
10. M. Sueki, G. A. Rinard, S. S. Eaton, and G. R. Eaton, *J. Magn. Reson. A* **118,** 173 (1996).
11. A. Sienkiewicz, K. Qu, and C. P. Scholes, *Rev. Sci. Instrum.* **65,** 68 (1994).
12. W. M. Walsh and L. W. Rupp, *Rev. Sci. Instrum.* **57,** 2278 (1986).
13. S. E. Bromberg and I. Y. Chan, *Rev. Sci. Instrum.* **63,** 3670 (1992).
14. S. Del Monaco, J. Brivati, G. Gualtieri, and A. Sotgiu, *Rev. Sci. Instrum.* **66,** 5104 (1995).
15. D. Kajfez, A. W. Glisson, and J. James, *IEEE Trans. Microwave Theory Tech.* **MTT-32,** 1609 (1984).
16. M. Jaworski and M. W. Pospieszalski, *IEEE Trans. Microwave Theory Tech.* **MTT-27,** 639 (1979).
17. S. J. Fiedziuszko and A. Jelenski, *IEEE Trans. Microwave Theory Tech.* **MTT-19,** 778 (1971).
18. T. Itoh and R. Rudokas, *IEEE Trans. Microwave Theory Tech.* **MTT-25,** 52 (1977).
19. M. W. Pospieszalski, *IEEE Trans. Microwave Theory Tech.* **MTT-27,** 233 (1979).
20. R. Isaacson, private communication.
21. A. Sienkiewicz, M. Jaworski, and C. P. Scholes, unpublished experimental results.
22. A. Karp, H. J. Shaw, and D. K. Winslow, *IEEE Trans. Microwave Theory Tech.* **MTT-16,** 818 (1968).
23. C. P. Poole, ''Electron Spin Resonance: A Comprehensive Treatise on Experimental Techniques,'' Chap. 8, Wiley–Interscience, New York, 1967.
24. Z. Czumaj, *Mol. Phys.* **69,** 787 (1990).